INFLUENCE OF PARASITIC CAPACITANCES ON THE POWER OUTPUT OF ELECTRET-BASED ENERGY HARVESTING GENERATORS

U. Bartsch, C. Sander, M. Blattmann, J. Gaspar, and O. Paul
Microsystem Materials Laboratory, Department of Microsystems Engineering - IMTEK,
University of Freiburg, Germany

Abstract: The power output of electrostatic energy harvesting generators is usually predicted using a widely accepted formulation derived by Boland et al. in 2003. However, this model neglects the effects caused by parallel parasitic capacitances, namely those built into the device itself and those introduced by the measurement setup. Even if such capacitances are in the pF range, they can cause a substantial power loss and the generator power cannot be realiably predicted. This paper describes the derivation and experimental validation of an extended analytical model, that takes parasitic capacitances into account.

Keywords: Micro energy harvesting, electret, parasitic capacitances

INTRODUCTION

Boland *et al.* have previously derived a formula for predicting the power output of electrostatic harvesting generators [1]. Their derivations for the output voltage V and the resulting power P, i.e.,

$$V = \frac{nfA_{max}2\sigma dR_L}{d + \varepsilon_E(g + 2nfA_{max}R_L\varepsilon_0)} \text{ and} \quad (1)$$

$$P = \frac{(2nfA_{max}\sigma d)^2 R_L}{[d + \varepsilon_E(g + 2nfA_{max}R_L\varepsilon_0)]^2} \quad (2)$$

are widely accepted and applied in the area of electret-based micro energy harvesting generators [2-4]. The model is based on the schematics shown in Fig. 1, where a time-dependent electret surface overlap $A(t)$ induces a current $I(t)$ through a resistive load R_L.

The parameters n, A_{max}, f, T, and σ denote the number of electret-counter-electrode-pairs, maximum overlap area, frequency, period T of $1/nf$, and surface charge density of the electret layer. The current $I(t)$ and the voltage $V(t)$ are rectangular signals. Therefore, the output power P is constant over time.

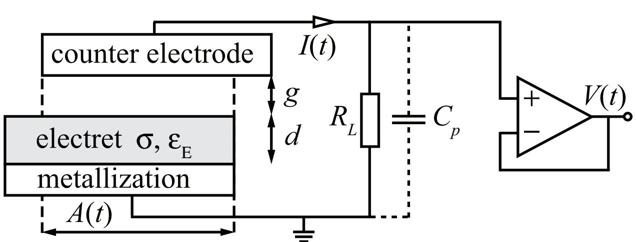

Fig. 1: Schematics of electret-based generator with load, parasitic capacitance and impedance converter.

However, this model neglects the effects caused by the parallel parasitic capacitances C_p indicated in Fig. 1. This capacitance is the sum of capacitance C_g built into the device itself and capacitances introduced by the measurement setup, C_m. Even for typical values of C_p in the pF range, C_p can cause a substantial power loss of the generator.

The deviation of the conventional model described by Eq. (2) from experimental data, based on the parameters given in Table. 1, is shown in Fig. 2. Both curves show the same qualitative behavior and the conventional model satisfactorily predicts the measurement results for small resistive loads. However, the measured maximum power output occurs at 300 MΩ, whereas the model predicts 5.5 GΩ. The two maximum powers deviate by a factor of about 15. The parasitic capacitances C_p, as illustrated in Fig. 1, are connected in parallel with the load resistor R_L. A certain fraction of $I(t)$ is lost for harvesting since it flows through C_p as a charge and discharge current. The charging time constant of the corresponding capacitance C_p in parallel with R_L is $\tau = C_p R_L$. For increasing resistive loads, τ increases. Above a certain load, the generator is not able to charge and discharge

Table 1: Parameters to compare calculations and experiment.

$n = 2$	$g = 155\ \mu m$	$A_{max} = 0.37\ cm^2$
$\varepsilon_E = 2.1$	$f = 20$ Hz	$\sigma = 0.93\ mC/m^2$
$f = 20$ Hz	$d = 9.5\ \mu m$	$\varepsilon_0 = 8.85\ 10^{-12} As/Vm$

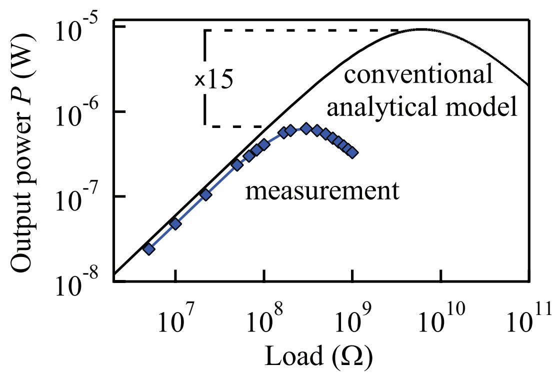

Fig. 2: Comparison of measured power output curve of an electret-based generator and results calculated using Eq. (2).

C_p during one period T and the output power reduces drastically.

The next section of this paper describes the derivation and experimental validation of an extended analytical model that takes C_p into account.

PARASITIC CAPACITANCES

In order to obtain an expression for the output voltage $V(t)$ as a function of R_L, the generator is modelled as a voltage source having a square signal and internal resistor R_i. The circuit model of the generator is shown in Fig. 3. The amplitude V_{max} of the voltage source and the value of R_i are obtained from Eq. (1). A graph of the generator voltage amplitude plotted as a function of R_L is shown in Fig. 4. The amplitude V_{max} is calculated as

$$V_{max} = \lim_{R_L \to \infty} V = \frac{\sigma d}{\varepsilon_0 \varepsilon_E} . \tag{3}$$

The internal resistance is obtained as

$$R_i = \frac{d + g\varepsilon_E}{2nfA_{max}\varepsilon_0\varepsilon_E} . \tag{4}$$

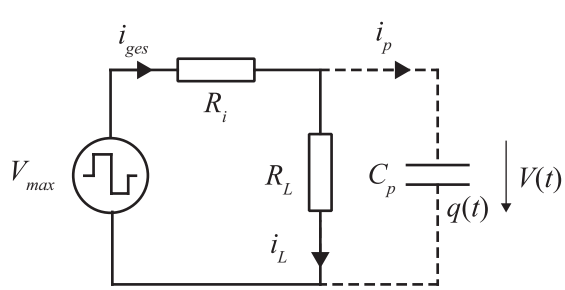

Fig. 3: Equivalent circuit representation of generator with square voltage and internal resistor R_i.

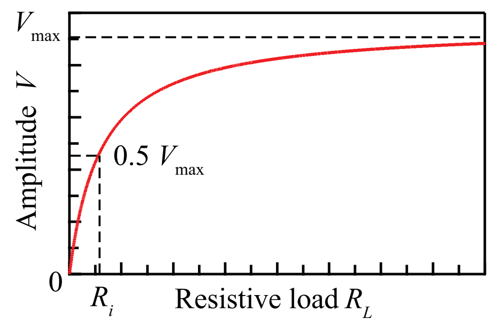

Fig. 4: Determination of the maximum generator voltage V_{max} and internal resistance R_i.

The model derived by Boland *et al.* can thus be described as a voltage devider of the internal source resistor R_i and the load R_L.

The circuit shown in Fig. 3, including the parasitic capacitance, can be described by the differential equation for the current i_p through C_p in terms of the charge $q(t)$ stored on C_p

$$\frac{dq(t)}{dt} = \frac{1}{R_i}\left(V_{max}(t) - \frac{q(t)}{C_p}\right) - \frac{q(t)}{C_p R_L} . \tag{5}$$

Here, the generator square voltage is given by

$$V_{max}(t) = \begin{cases} \dfrac{\sigma d}{\varepsilon_0 \varepsilon_E}, \ 0 \le t < T/2 \\ -\dfrac{\sigma d}{\varepsilon_0 \varepsilon_E}, \ T/2 \le t < T \end{cases} \tag{6}$$

and the boundary condition for the steady state is

$$q(0) = -q(T/2) . \tag{7}$$

The solution of the differential equation can be obtained analytically in the time intervall [0; T/2]. The voltage drop over R_L is $V(t) = q(t)/C_p$. An important quantity is the amplitude of the output voltage, V_{amp}, at $t = kT/2$, with k any positive integer given by

$$V_{amp} = \frac{R_L}{R_i + R_L} V_{max} \tanh\left(\frac{R_i + R_L}{4C_p nfR_iR_L}\right). \tag{8}$$

The hyperbolic tangent function is appended to the equation as a result of the parasitic capacitance C_p. If C_p is neglected, Bolands formula of the voltage divider is recovered.

The effective power of the generator can be calculated as the average of the time dependent output power,

$$P = \frac{2}{T}\int_0^{T/2} V(t)^2/R_L \quad (9)$$

$$= \frac{R_L V_{max}^2}{(R_i + R_L)^3} \times \left(R_i + R_L - 4C_p nfR_iR_L \tanh\left(\frac{R_i + R_L}{4C_p nfR_iR_L}\right)\right).$$

Again, if parasitic capacitances are neglected, the hyperbolic tangent asymtotically approaches 1 and Eq. (9) reduces to Eq. (2).

ELECTRET-BASED DEMONSTRATOR

An electret-based rotational energy harvesting generator was implemented in order to evaluate the accuracy of the new analytical model. The demonstrator setup is shown in Fig. 5. The counter electrode and the electret are placed facing each other, seperated by the gap distance g. The gap can be varied using a linear stage in the µm range and is measured using a laser-deflection detector. The time variation of the overlapping area is realized by rotating the patterned electret chip with respect to the counter electrode chip using a DC stepper motor with frequencies up to 100 Hz.

Both electret and counter electrode chips are shown in Fig. 6. The counter chip contains four metal electrodes processed on a Pyrex substrate. Each of these regions is electrically connected to the opposite counterpart, resulting in two separate counter electrodes, into which charge is induced alternately. The electret chip consists of a Cytop® type CTL-809M (Asahi Glass, Tokyo, Japan) electret layer on top of a metallization. The chips are charged using a corona discharge [5]. The resulting surface charge density is measured using an electrostatic voltmeter. A two-dimensional scan of the measured surface potential of the used chip is shown in Fig. 7. The average surface charge density σ is 0.93 mC/m^2.

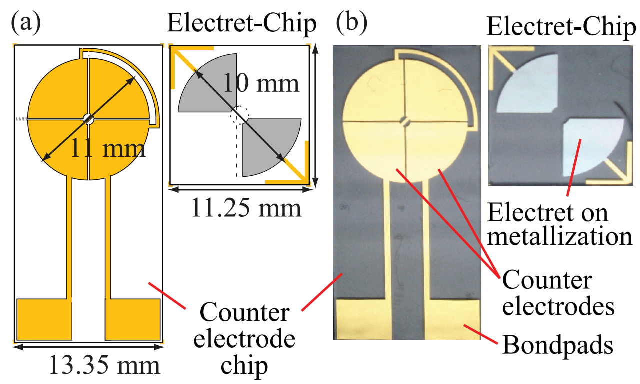

Fig. 6: (a) Schematics and (b) photograph of counter electrode and electret chips.

The output power of the demonstrator is characterized by measuring the output voltage $V(t)$ across a certain load resistor using an operational amplifier (OPA), as shown in Fig. 1. The OPA, with an input impedance of $10^{14}\ \Omega$, is used in a voltage follower configuration to decouple the measurement circuit from the demonstrator. A high input impedance amplifier is necessary, since R_L values can be in the GΩ range.

EXPERIMANTAL VALIDATION OF THE MODEL

For the practical validation of the new model, measurements were performed with the demonstrator using the parameters in Table. 1. Three different configurations of parasitic capacitances are investigated: (i) the demonstrator without additional capacitance, (ii) an additional capacitance of 22 pF in parallel with R_L, and (iii) 82 pF in parallel with R_L. The experimental results along with those obtained using

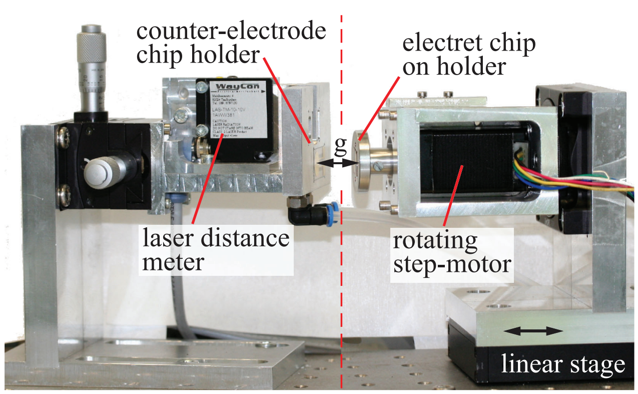

Fig. 5: Electret-based rotational energy harvesting demonstrator.

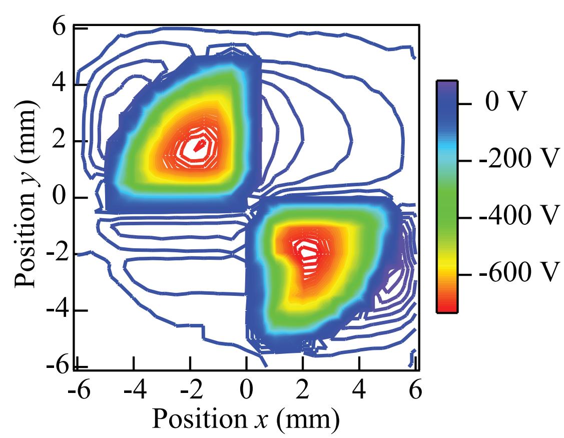

Fig. 7: Two-dimensional scan of the surface potential of the electret chip.

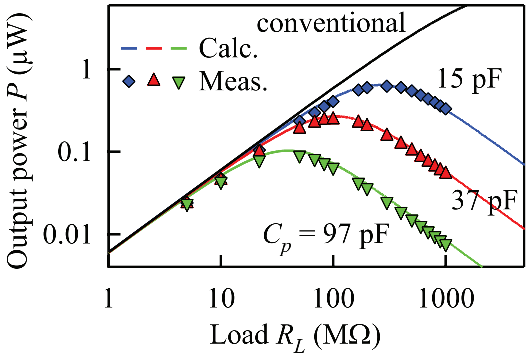

Fig. 8: Measured and calculated output power of the demonstrator for various parasitic capacitances as a function of the load resistor.

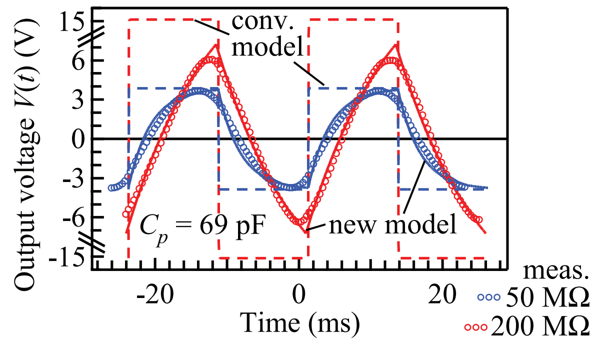

Fig. 9: Measured and calculated output voltage of the demonstrator for two different load resistors.

the conventional model are shown in Fig. 8, plotted in logarithmic scale. The analytical model matches all the the measurements very accurately. In contrast, the conventional model only describes the measurements results for small loads. Furthermore, the absolute intrinsic capacitance of an energy harvesting generator without additional capacitor can be determined from this type of measurement. An intrinsic capacitance of 15 pF was thus determined for the current demonstrator.

In addition to the prediction of the effective power, the time dependent output voltage $V(t)$ of the generator is of interest. Whereas the conventional model only allows for modeling square-wave signals as the output voltage, the extended model enables to include typical charge and discharge curves of the capacitor C_p. Both measured and calculated signals of the output voltage are shown in Fig. 9 for the parameters R_L = 50 MΩ and 200 MΩ. An additional capacitor of 47 pF was placed in parallel with the load resistor. The total parasitic capacitance used in the calculations was 62 pF.

For R_L = 50 MΩ, the measured curve and the calculations just reach the saturation value, which is also predicted by the conventional model. With increasing resistive load, the demonstrator is not able to completely charge C_p during one period T. For a load of 200 MΩ, the amplitude of the measured voltage is 5.8 V. The predicted amplitude using the conventional model is 15 V and thus almost three times larger. The amplitude calculated using the new model is 7.2 V, and therefore much closer to the measurement results. The remaining disagreement is attributed to the neglect of fringing electric fields at the edges of the electret areas, which result in a rounded curve instead of one with sharp kinks.

CONCLUSIONS

An extended analytical formula for the power output of electrostatic energy harvesting devices is derived. The formulation is based on an expression derived by Boland *et al.* in 2003 and takes the effect of parasitic capacitances on the output power into account. The newly derived model was experimentally verified using an electret-based rotational harvesting demonstrator.

ACKNOWLEDGMENTS

This study is part of the PhD program “Micro Energy Harvesting” funded by the German Research Foundation DFG under project no. GRK 1322.

REFERENCES

[1] Boland J, Chao Y, Suzuki Y, and Tai Y.C 2003 Micro Electret Power Generator *Tech. Dig. IEEE MEMS 2003* 538-541

[2] Naruse Y, Matsubara N, Mabuchi K, Izumi M, Honma K 2008 Electrostatic Micro Power Generator from Low Frequency Vibration such as Human Motion *Proc. PowerMEMS 2008* 19-22

[3] Arakawa Y, Suzuki Y, Kasagi Y 2004 Micro Seismic Power Generator Using Electret Polymer Film *Proc. PowerMEMS 2004* 187-190

[4] Tsutsumino T, Suzuki Y, Kasagi N, Tsurumi Y 2005 High-Performance Polymer Electret for Micro Seismic Generator *Proc. PowerMEMS 2005* 9-12

[5] Bartsch U, Gaspar J, Paul O 2008 Characterization of the Charging and Long-Term Performance of Cytop Electret Layers for MEMS Applications *Proc. MRS Fall Meeting* 1135-BB08-17